ISTITUTO NAZIONALE DI GEOFISICA E VULCANOLOGIA

Site characterization report at the seismic station IT.BRH – Brisighella (RA)

Report di caratterizzazione di sito presso la stazione sismica IT.BRH – Brisighella (RA)

Working Group **Geology:** Paolo MANGANELLO, Sara LOVATI **Geophysics**: Rodolfo PUGLIA, Giulio BRUNELLI, Alessio LORENZETTI, Sara LOVATI, Paolo MANGANELLO, Marco MASSA	Date: December 2021
Subject: **Final report illustrating the site characterization for seismic station IT.BRH**	

Convenzione DPC-INGV 2019-21, All. B2- WP1, Task 2: "Caratterizzazione siti accelerometrici" (Coord.: G.Cultrera, F. Pacor)
Cite as: Working group INGV "Agreement DPC-INGV 2019-21, All. B2- WP1, Task 2", (2021). Site characterization report at the seismic station *IT.BRH – Brisighella (RA).* http://hdl.handle.net/2122/15018

INDEX

INTRODUCTION

In this report we present the geological setting and the geophysical measurements and results obtained in the framework of the 2019-2021 agreement between INGV and DPC, called *Allegato B2: Obiettivo 1 - TASK 2: Caratterizzazione siti accelerometrici (Responsabili: G. Cultrera, F. Pacor)* for the site characterization of station IT.BRH (Brisighella).

Location and coordinates are reported in Table 1.

Table 1

CODE	NAME	LAT [°]	LON [°]	ELEVATION [m]
IT.BRH	Brisighella (RA)	44.207610 *	11.763964 *	144 **
ADDRESS	Via Siepi, 39, 48013 Brisighella (RA), Italy			

* Coordinates from ITACA (Nov. 2021) ** Elevation from CTR 5k Regione Emilia-Romagna

A. Geological setting

A1. TOPOGRAPHIC AND GEOLOGICAL INFORMATION

Topographic information related to the site are reported in Table 2. Table 3 summarizes all available geological maps from literature for geological analyses.

Table 2

Topography	Description	Topography Class	Morphology Class
	Flat surfaces, isolated slopes and reliefs with slope i ≤ 15°	T1	Valley edge (VE)

Table 3

Geological map	Source	Scale
IT.BRH	Geological Map of Italy (CARG Project), sheet 239 (Faenza)	1:50.000
IT.BRH	Geologic Technical Map, Comune di Brisighella - Seismic Microzonation	1:10.000

In Table 4 Geological, Lithological and Lithotechnical Units (according to Seismic Microzonation classification; Technical Commission SM, 2015) are described and are concerned to the maps of following chapters. The term "original" means the result comes from a preexisting cartography (Table 3); the term "deduced" means the result comes from an interpretation of a preexisting cartography according to the nomenclature of corresponding cartography.

Table 4

GEOLOGICAL UNITS		**LITHOLOGICAL UNITS**		**LITHOTECHNICAL UNITS**	
Geological Map of Italy 1:50.000 (CARG Project), sheet 239 (Faenza) *original*		Amanti *et al.* (2008) *deduced*		(MZS) *original*	
code	**description**	**code**	**description**	**code**	**description**
AES$_7$	Villa Verucchio Subsynthem	B4	Mixed clay-sand-gravel	CLtf	Gravelly or sandy clay
AES$_8$	Ravenna Subsynthem	B4	Mixed clay-sand-gravel	MLtf	Clayey or silty fine sand
FMA$_{10}$	Marnoso-Arenacea Formation (Dovadola Member)	A10	Pelite-sandstone alternance	ALS	Alternation of lithotypes, stratified
				GCtf	Gravel-sand-clay mixture

Convenzione DPC-INGV 2019-21, All. B2- WP1, Task 2: "Caratterizzazione siti accelerometrici" (Coord.: G.Cultrera, F. Pacor)
Cite as: Working group INGV "Agreement DPC-INGV 2019-21, All. B2- WP1, Task 2", (2021). Site characterization report at the seismic station *IT.BRH – Brisighella (RA).* http://hdl.handle.net/2122/15018

A2. GEOLOGICAL MAP

In Figure 1 Geological Map is reported in a 1 $km \times 1$ km square around the station.

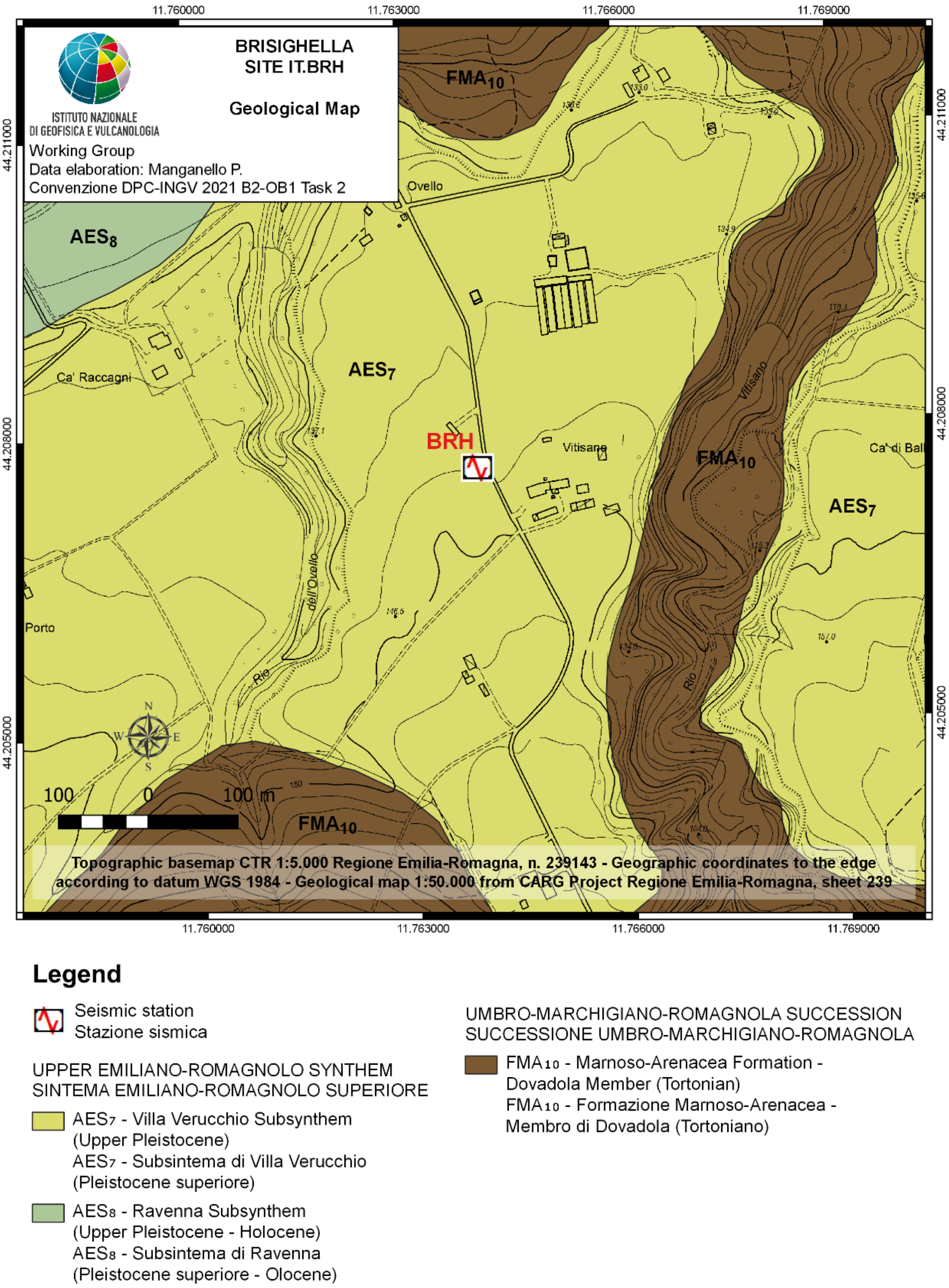

Figure 1: Geological map of seismic station IT.BRH. Scale 1:5.000. The geological units are established according to the nomenclature of the Geological Map of Italy 1:50.000 (CARG Project – sheet 239).

A3. LITHOLOGICAL MAP

In Figure 2 Lithological Map is reported in a 1 $km \times 1$ km square around the station.

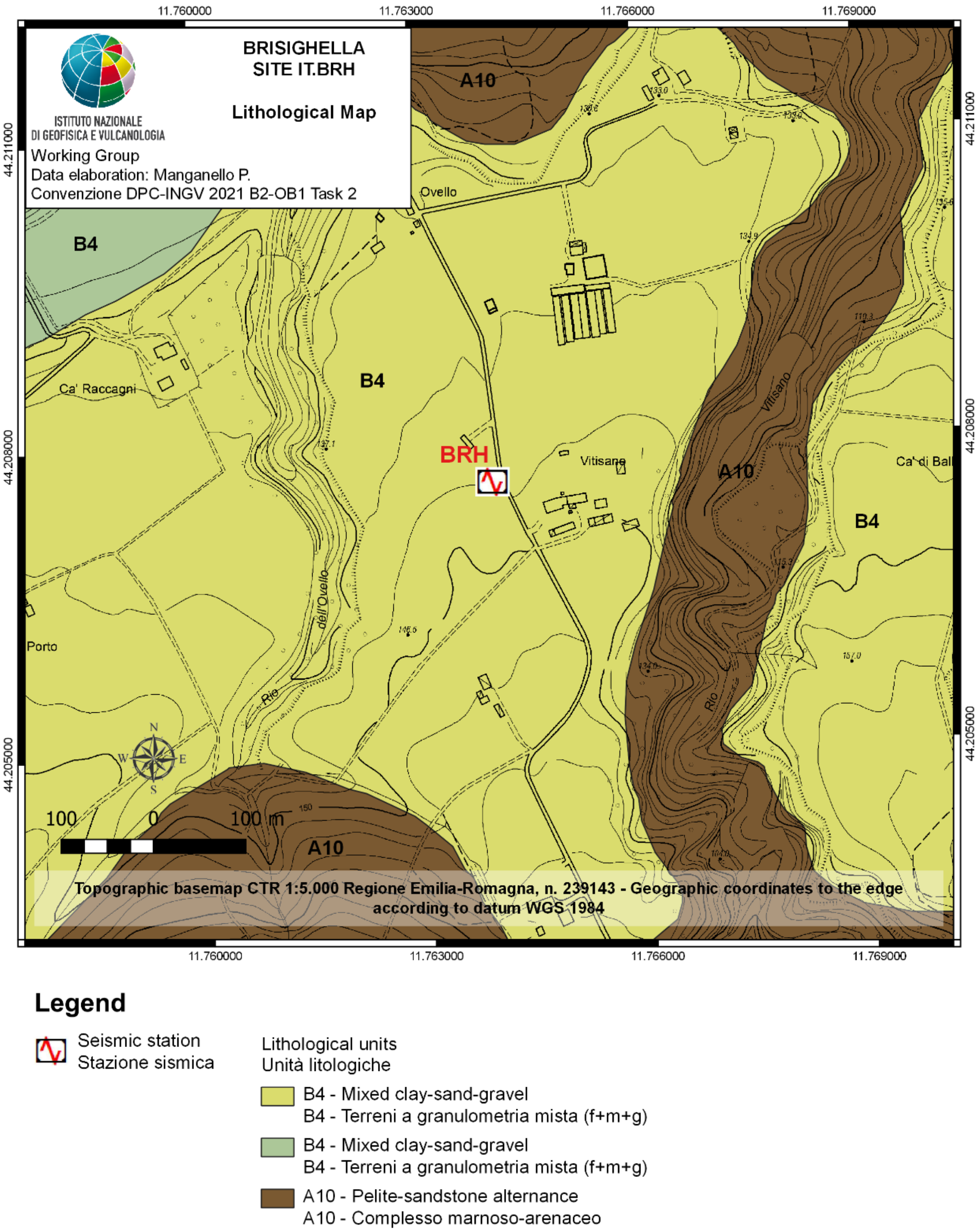

Figure 2: Lithological map of the seismic station IT.BRH. Scale 1:5.000. The codes of the lithological units are assigned according to the nomenclature of the Lithological map of Italy ISPRA 1:100.000 (Amanti *et al.*, 2008).

A4. LITHOTECHNICAL MAP

In Figure 3 Lithotechnical Map is reported in a 1 $km \times 1$ km square around the station.

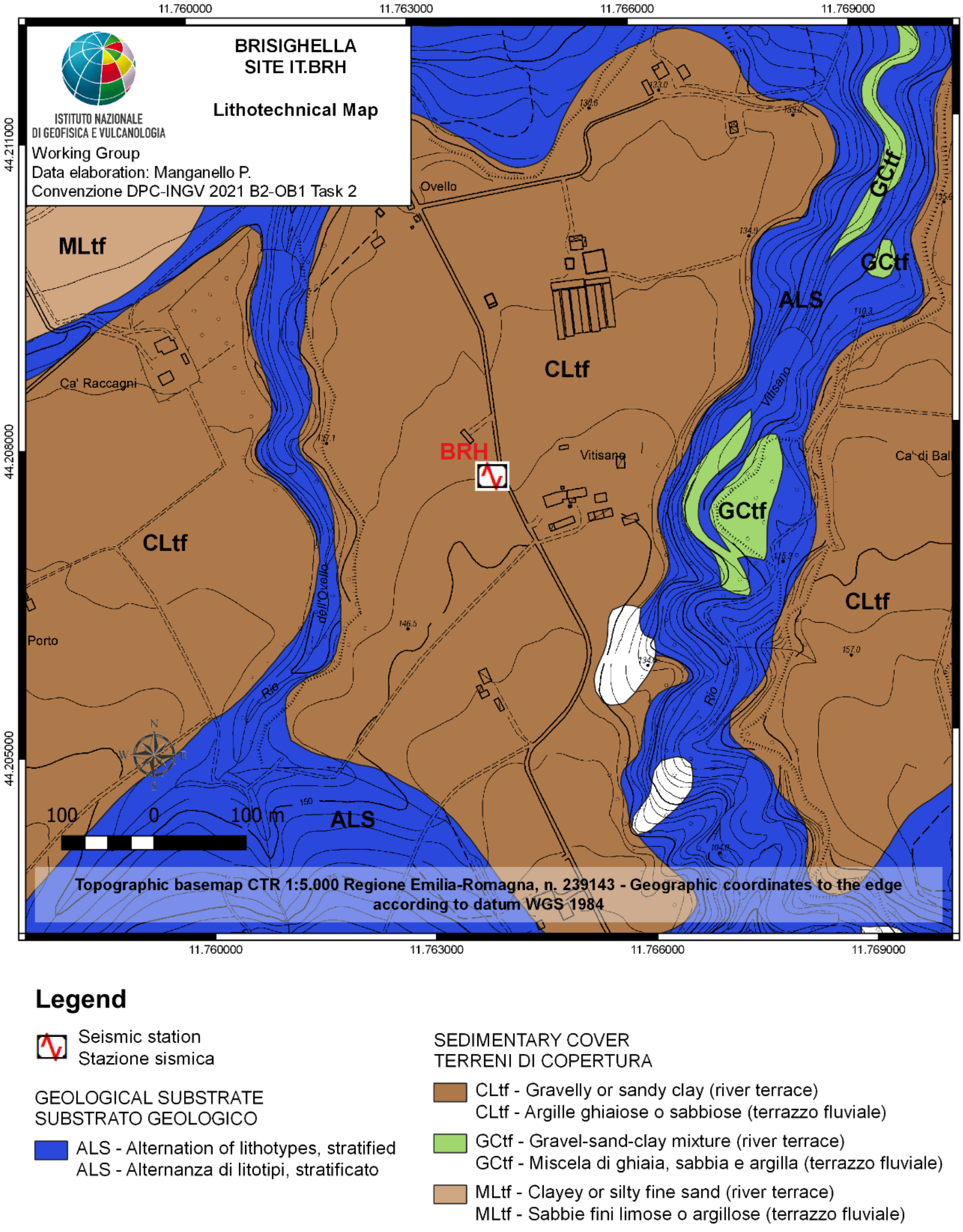

Figure 3: Lithotechnical map of the seismic station IT.BRH. Scale 1:5.000. The lithotechnical units are assigned according to the nomenclature of Seismic Microzonation (Technical Commission SM, 2015).

A5. SURVEY MAP

Figure 4 shows the Survey Map reporting both previous investigations and geophysical surveys conducted by INGV Working Group.

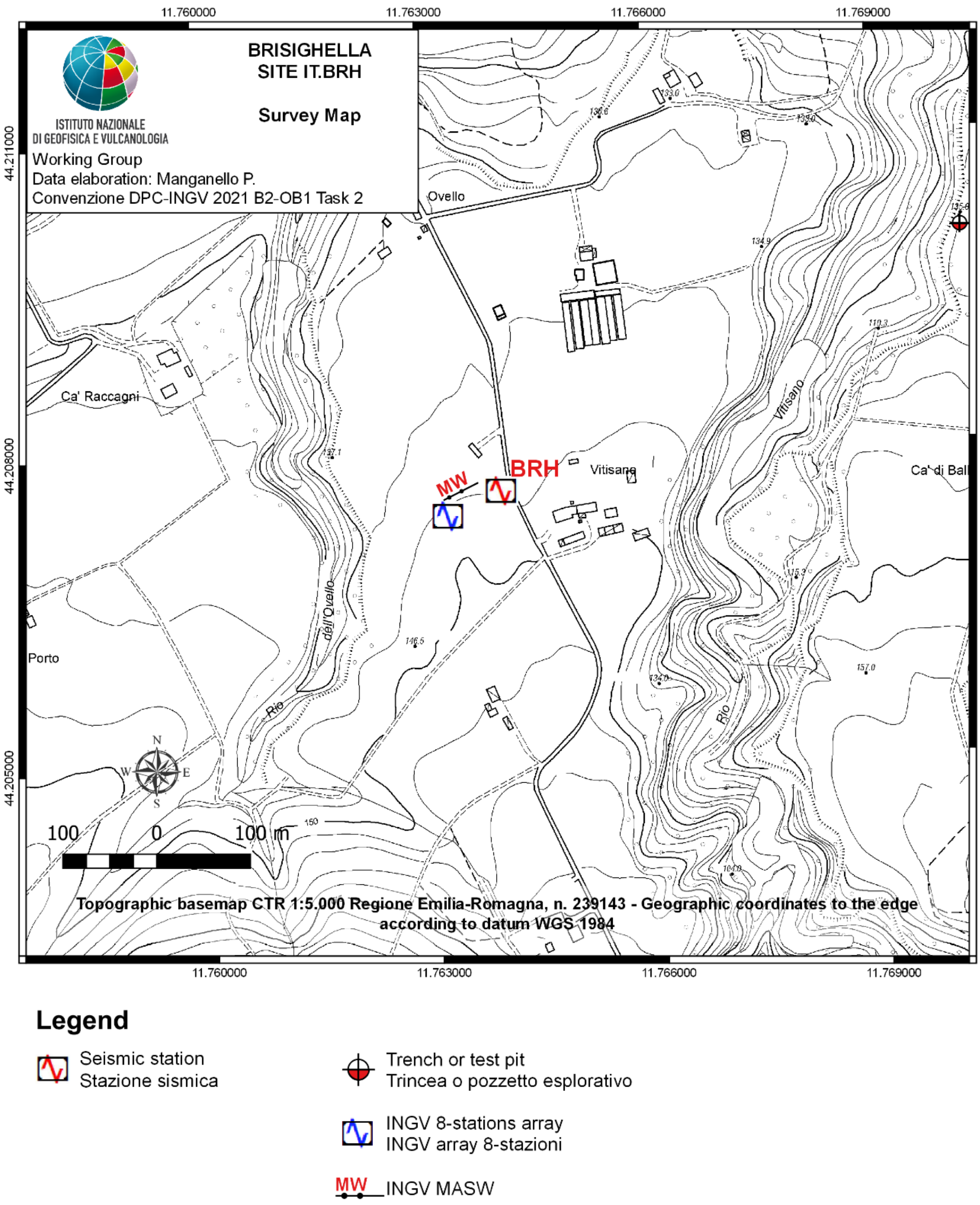

Figure 4: Map of the surveys in the surroundings of the station IT.BRH. Scale 1:5.000.

A6. GEOLOGICAL MODEL

6.1 General description

The seismic station IT.BRH is installed in the municipality of Brisighella (Ravenna Province, Northern Italy), further south to the town center. The municipality of Brisighella is located in the lower Lamone river valley.

The geology of Brisighella area is related to the first phase of the Messinian salinity crisis, which has produced the Vena del Gesso basin, a thrust-top basin in the western Romagna Apennines (Northern Apennines) constituted mainly by primary selenitic gypsum, gypsarenites and gypsumrudites. This basin was delimited to the North by a syn-sedimentary growing anticline correlated to the thrust, and hinterland-ward it was bordered by the advancing Apenninic fold and thrust belt. After the end of the deposition of gypsum, the area has been characterized by massive submarine landslides that caused the dismantlement of the gypsum formation and the deposition of the Resedimented Lower Gypsum unit (Montanari *et al.*, 2007; Lugli *et al.*, 2015). The Marnoso - Arenacea Formation (Langhian - Tortonian), which is characterized by deep-water sandstones and marls turbidites mainly constituted by detritus derived from the erosion of Alps, represents the substratum of the Vena del Gesso basin. The Marnoso - Arenacea Formation is entirely detached from the underlying Meso-Cenozoic carbonates. The Messinian evaporites have been subjected to local sub-aerial dissolution and erosion prior to deposition of the unconformable Colombacci Formation (Late Messinian), which is mainly represented by marls and clays. At the end of the Messinian salinity crisis the deposition of the post-evaporitic succession of the Padano-Adriatico margin started (e.g., the Argille Azzurre Formation (Lower Pliocene - Lower Pleistocene), primarily constituted by clays and marly clays deposited in relatively deep marine environment) (Roveri *et al.*, 2003; Simoni *et al.*, 2003; Montanari *et al.*, 2007).

The Quaternary deposits are represented by the continental deposits of the Emiliano-Romagnolo Supersynthem (Middle Pleistocene - Holocene), which has a thickness of a few tens of meters in the area of the Apenninic margin.

6.2 Geological section

The WSW-ENE oriented geological section is reported and highlights the geological and structural setting of the IT.BRH site. The trace with location of the section is reported as a blue line in the geological map (Fig. 5 upper left).

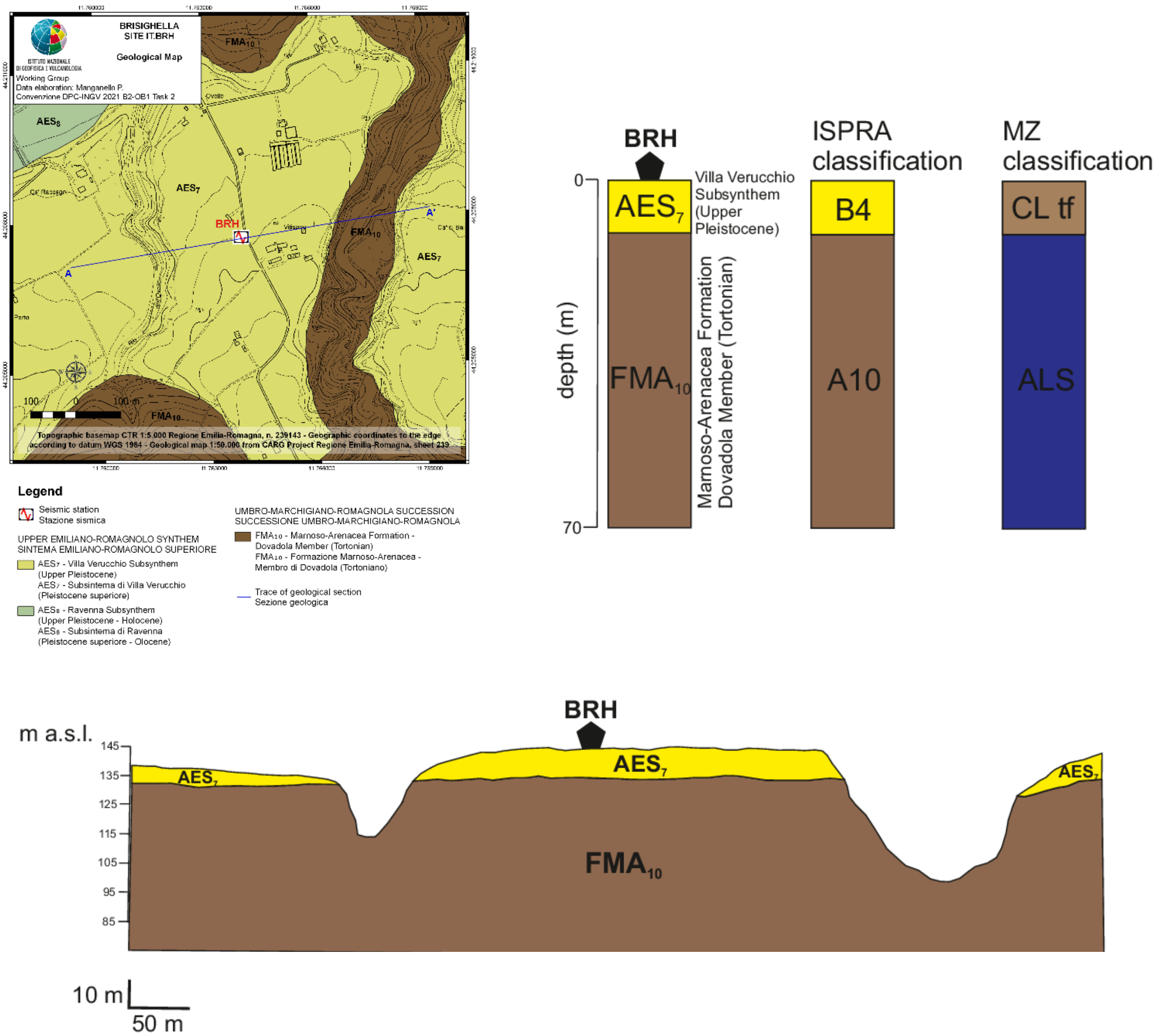

Figure 5: Upper left: Geological map of the study area where is installed IT.BRH seismic station. Upper right: Geological section. Bottom: Subsoil model for the site.

6.3 Subsoil model

The geological description reported from the surface to the bottom is described in the following part. There are not boreholes in the surroundings of the IT.BRH seismic station and a subsoil model is built up to a depth of 70 *m* on the basis of geological information (Figure 5 bottom).
The stratigraphic succession starts with the Villa Verucchio Subsynthem (AES_7 – Upper Pleistocene), which belongs to the Upper Emiliano-Romagnolo Synthem and is represented by deposits of river terrace. The thickness of this unit is about 10 meters.
Below an unconformity separates the Villa Verucchio Subsynthem from the Dovadola Member (FMA_{10}) of the Marnoso-Arenacea Formation (Umbro-Marchigiano-Romagnola Succession), which is characterized by an alternation of sandstones-pelites with marls deposited during the Tortonian. The maximum thickness of the Dovadola Member is 150 *m*.

B. V_S profile

B1. GEOPHYSICAL INVESTIGATIONS

Geophysical measurements executed nearby the station BRH of the network IT (PCM-DPC, 1972) consist in ambient-vibration measurements in both single-station and 2D array configuration (Figure 6) that provide results in terms of resonance frequency of the soil deposits and in terms of dispersion curves of surface waves. Furthermore, a Multi-channel Analysis of Surface Waves survey (MASW) is performed, which provides results in terms of dispersion curves of surface waves. These curves are inverted to obtain a shear-wave velocity (V_S) profile that, together with the geological study at section A, is suitable for assigning the soil class according to the current Italian seismic code (NTC18) and Eurocode (EC8).

Figure 7 shows the location of the accelerometric station IT.BRH (Latitude 44.207610, Longitude 11.763964 WGS84) installed on a concrete pillar inside an ENEL transformer cabin (n. 81365, name: Vitisano) in the municipality of Brisighella (RA).

Seismic noise is acquired using 8 Reftek-130 24-bits recording systems equipped with short-period Lennartz LE-3D/5s sensors and GPS timing (Figure 7). The sampling rate is fixed to 200 *Hz*, while the gain is set as “high”. Ambient noise recordings have a minimum duration of 1 hour. The array geometry (Figure 8) is chosen in order to have a good coverage of both azimuths and inter-station distances, the latter between the minimum (less than 10 *m*) and the maximum (about 30 *m*). These ranges allow the analysis of a range of wavelengths that guarantee sufficient shallow resolution in order to estimate the $V_{S,30}$ and the site-class according to current building codes (i.e. NTC18 and EC8).

Figure 6: Map of the geophysical measurements performed at the IT.BRH site. The yellow place-markers indicate the geometry used for 2D array in passive configuration. The red line indicates the line of 24 geophones used for MASW. The red triangle indicates the IT.BRH accelerometric station (image from Google Earth http://www.earth.google.com).

Figure 7: Upper left: accelerometric station IT.BRH installed in Brisighella (RA). Bottom left: ENEL transformer cabin where the station IT.BRH is installed and MASW acquisition line. Upper right: single station ambient noise measurement. Bottom right: 2D passive ambient noise array installed close to the IT.BRH station.

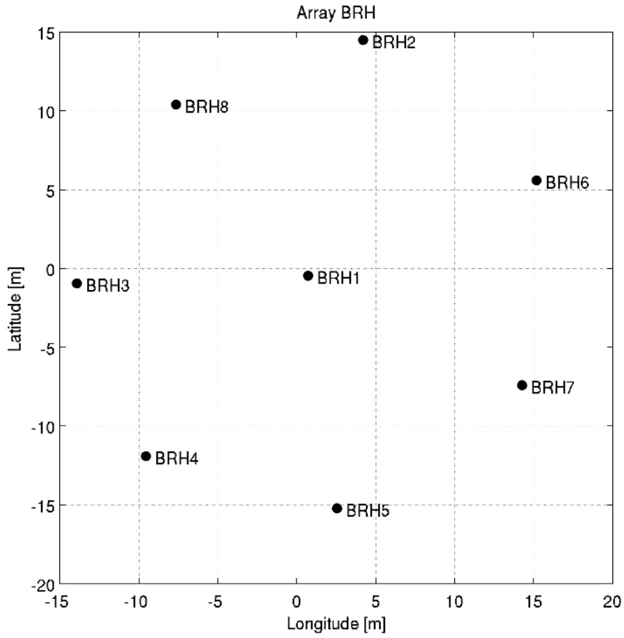

Figure 8: Array geometry.

The first step of the analysis consists in a visual inspection of the recordings at each station of the array. In particular, in order to identify malfunctioning and to select signal windows suitable for the surface wave analysis, the quality of the recording is evaluated analyzing the signal stationarity in the time domain, the relevant unfiltered Fourier spectra, and the H/V variation over time. Figures 9 and 10 provide graphical results about station BRH7.

It is common practice during surface wave investigation to verify the reliability of the one-dimensional site structure assumption (Aki, 1957; Okada, 2003). For this reason, we estimated the HVSR at each station of the array and the stability of HVSR among the array stations has been verified. Figure 11 depicts the HVSR assumed as representative for the array.

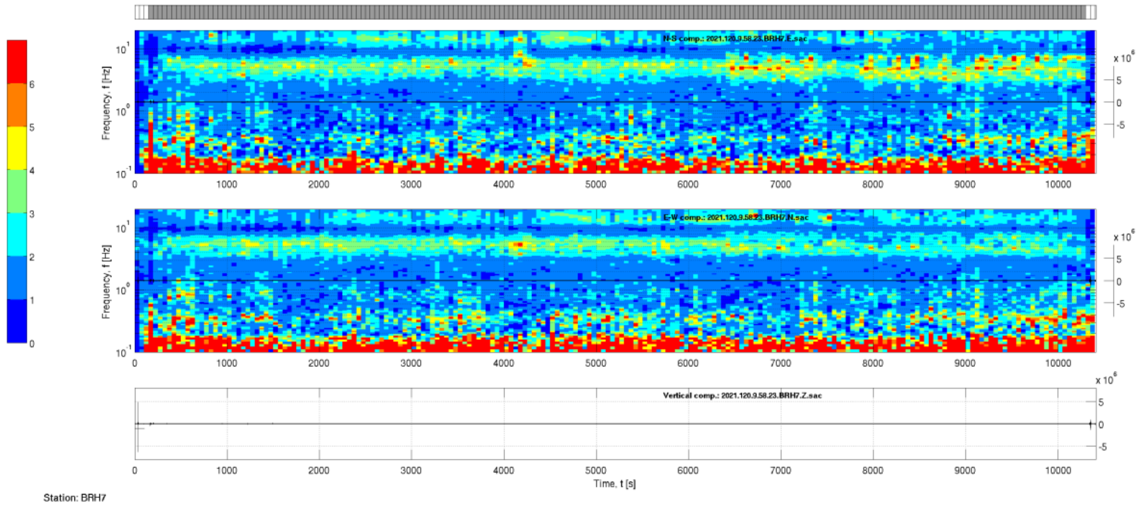

Figure 9: HVSR versus time (top and central panel for the NS and EW component, respectively) and corresponding time-histories.

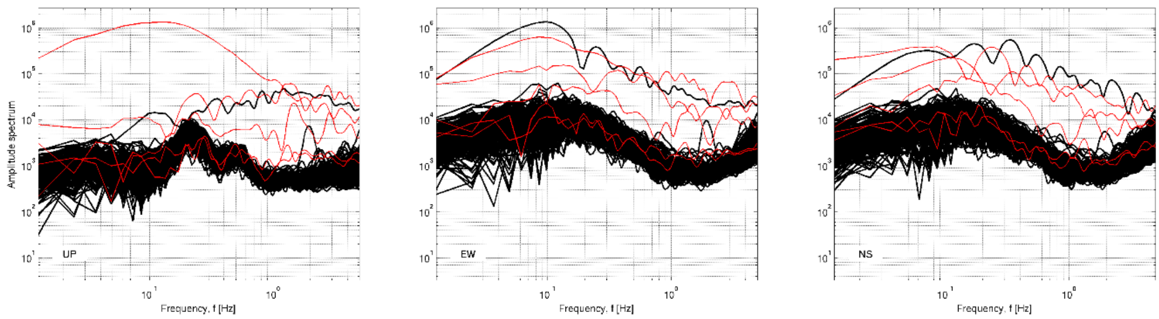

Figure 10: Fourier spectra for each noise window (left: Vertical, center: EW, right: NS); red spectra are excluded from HVSR analysis.

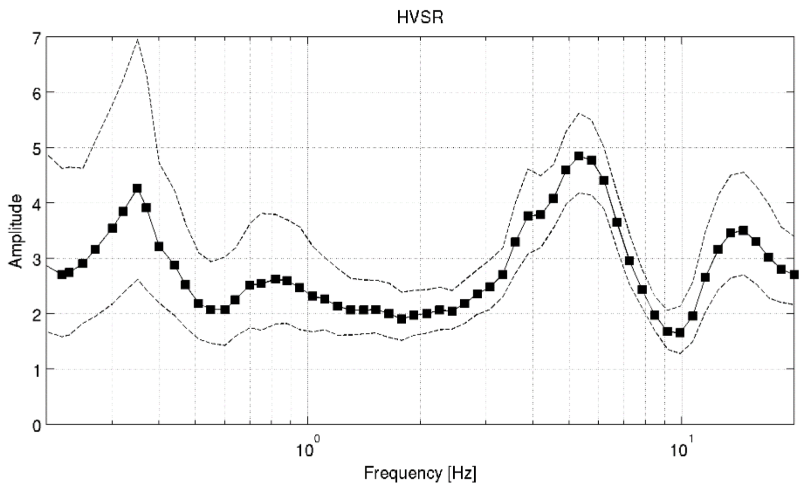

Figure 11: HVSR representative for the array. Dashed lines represent +/- one standard deviation.

The Rayleigh-wave dispersion curve is estimated by analyzing the vertical component of the recorded seismic noise. In particular, the Extended Spatial Auto-Correlation (ESAC; Ohori *et al.*, 2002; Okada, 2003) and the frequency-wavenumber (F-K; Lacoss *et al.*, 1969; Capon, 1969) methods are adopted. Further details about the combined use of ESAC and F-K approaches can be found in Parolai *et al.* (2006).

Both analyses use 120 synchronized signal windows of 60 *s* each, extracted from recordings within the UTC date-time interval 2021-04-30T10:26:00 – 2021-04-30T12:26:00, avoiding time periods affected by local disturbance.

The ESAC Rayleigh-wave dispersion curve is obtained by minimizing the root-mean-square (RMS) of the differences between experimental and theoretical Bessel functions (Figure 12). Values differing by more than two standard deviations from those estimated by the best fitting functions are automatically discarded (red circles in Figure 12) and the procedure is repeated iteratively. For this data set, data are also discarded whenever the inter-station distance is 2 times longer than the relevant wavelength. Figure 13 shows the Rayleigh-wave dispersion curve estimated using the ESAC approach.

The F-K analysis allows checking on the noise source distribution. One of the basic assumptions for the application of the ESAC method is indeed that the seismic noise wavefield is nearly isotropic. Figures 14 and 15 show results of the F-K analysis in terms of power density function for several frequencies using the Maximum Likelihood Method (MLM) and the Beam Forming (BF) respectively.

The MASW survey is based on the simultaneous analysis of surface wave traces recorded by an equally spaced array of receivers (Foti *et al.*, 2017). The used acquisition device has been a Geometrics Geode seismograph (24 channel) and the acquisition line consisted in 24 vertical geophones (4.5 *Hz* natural frequency) with a receiver spacing of 3 *m* (Figure 7). Two shots have been performed with offsets equal to 5 *m* and 10 *m*. The used source has been a sledgehammer striking on a metal plate. The chosen data acquisition parameters have been a time window of 2 *s* and a sampling frequency of 2 *kHz*.

The Rayleigh-wave dispersion curve (Figure 17) is estimated by picking the maximum amplitudes on the phase velocity – frequency plot obtained from recorded data.

Figures 16 and 17 respectively show a fairly good agreement between the ESAC and the F-K in the frequency range 10-12 *Hz* and a good agreement between the ESAC and the MASW in the whole frequency range.

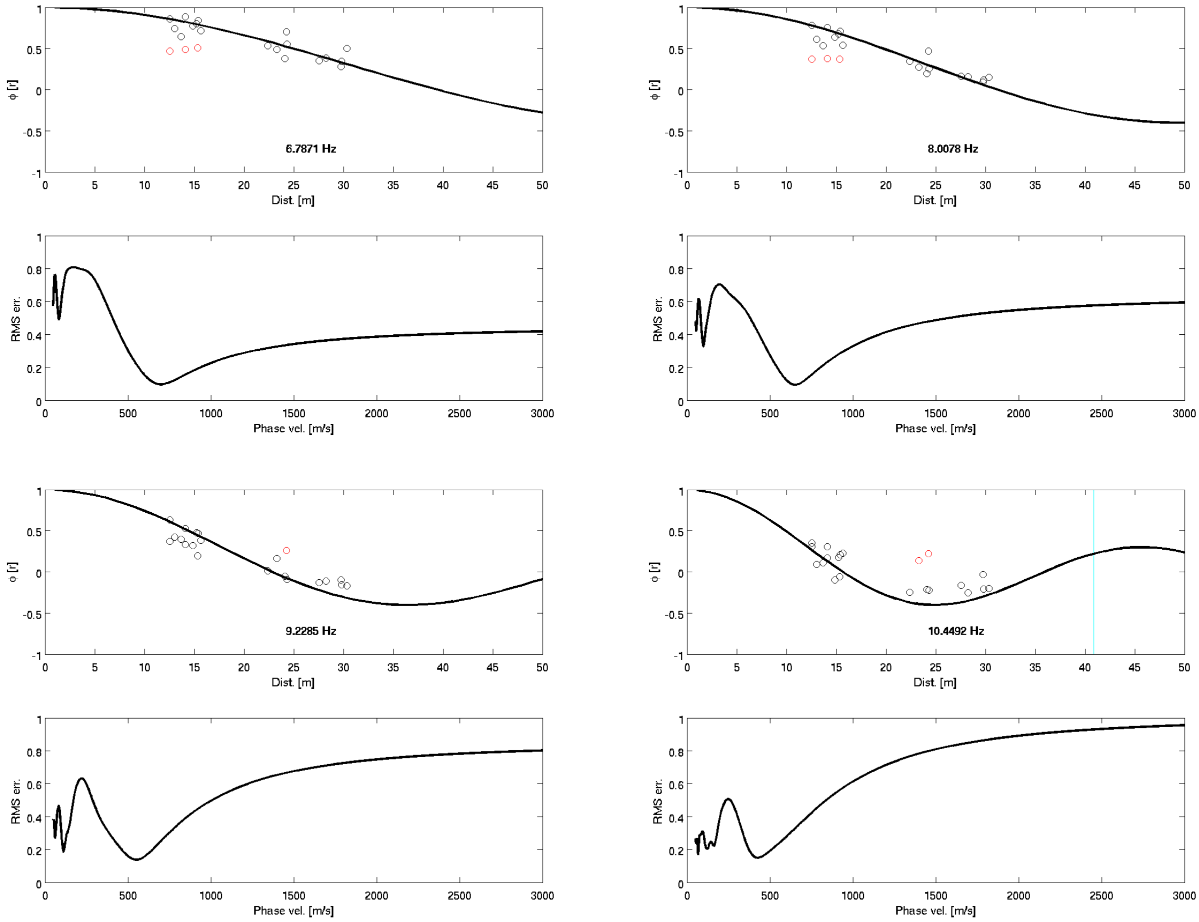

Figure 12: Experimental space-correlation function values versus distance (circles) for different frequencies. The red circles indicate values that are discarded. The black lines depict the estimated space-correlation function values for the phase velocity that furnishes the best fit to the data. The bottom panels show the relevant root-mean-square errors (RMS) versus phase velocity tested.

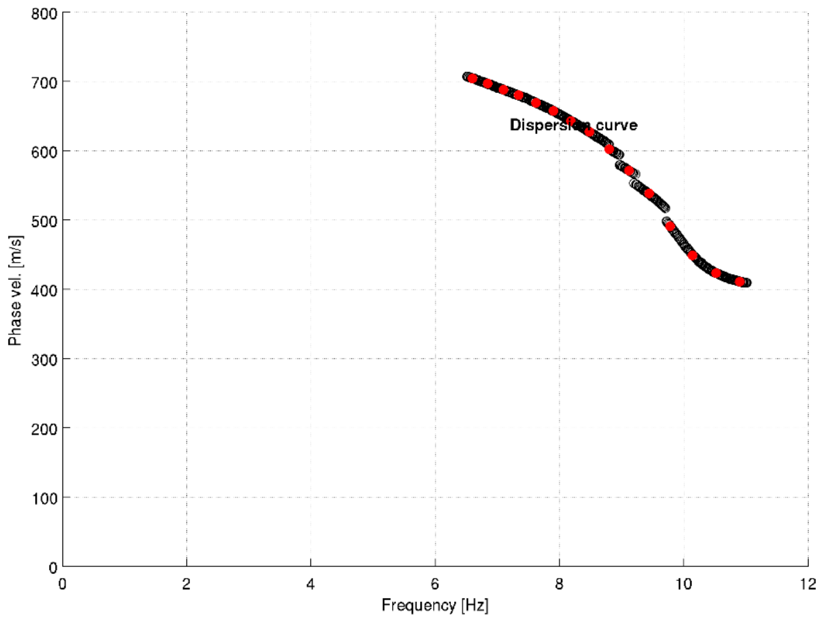

Figure 13: Rayleigh-wave dispersion curve from ESAC; red-filled circles represent values potentially used for inversions.

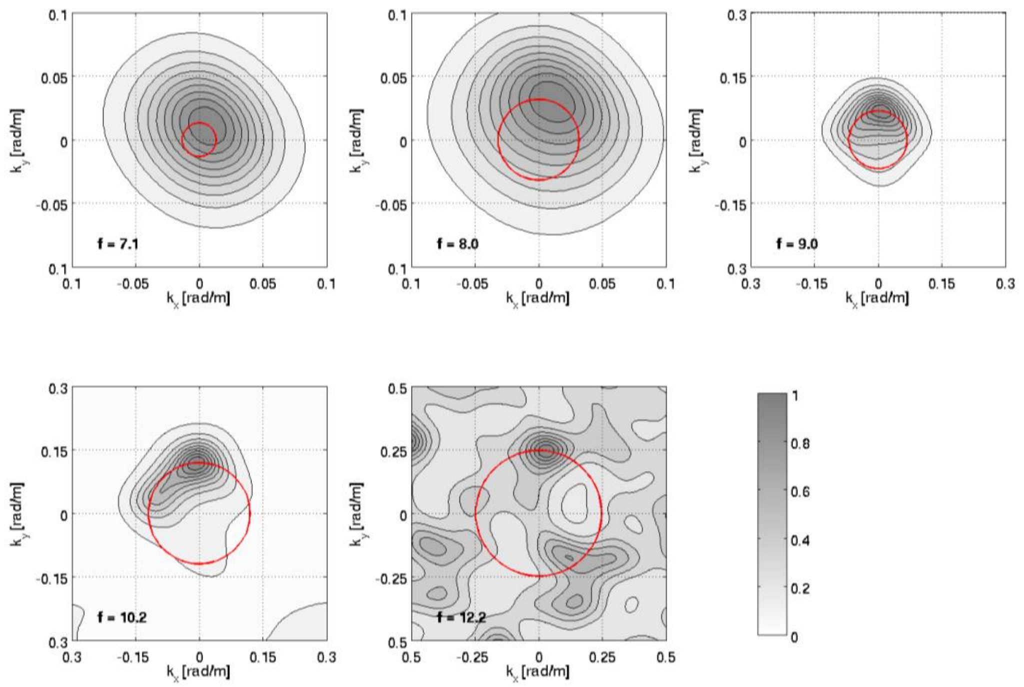

Figure 14: F-K power density function (Maximum-Likelihood Method) at selected frequencies.

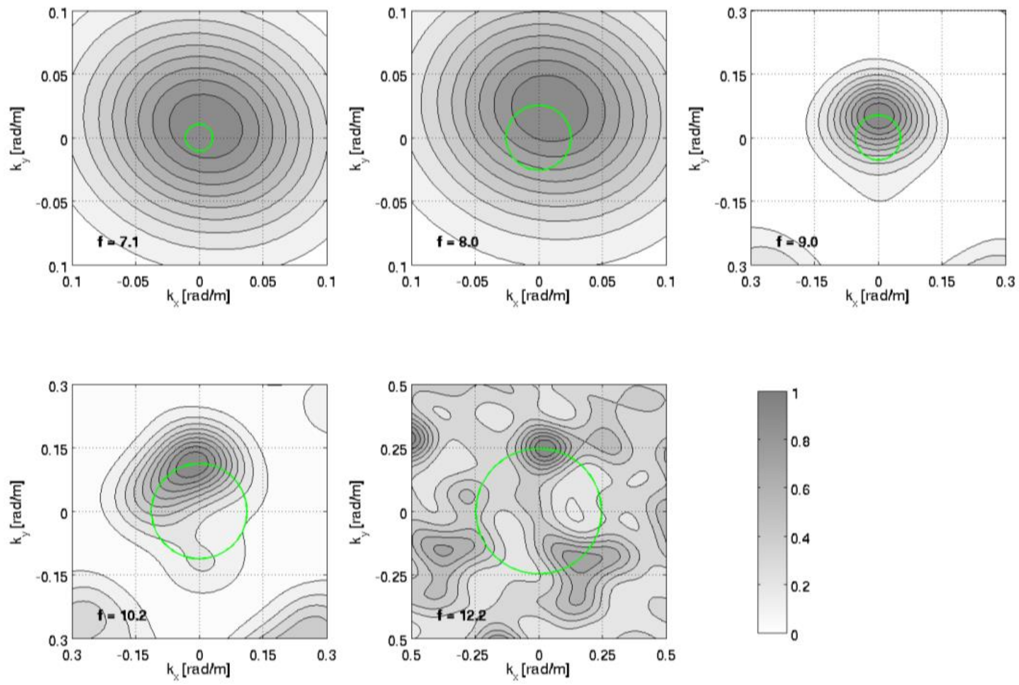

Figure 15: F-K power density function (Beam Forming) at selected frequencies.

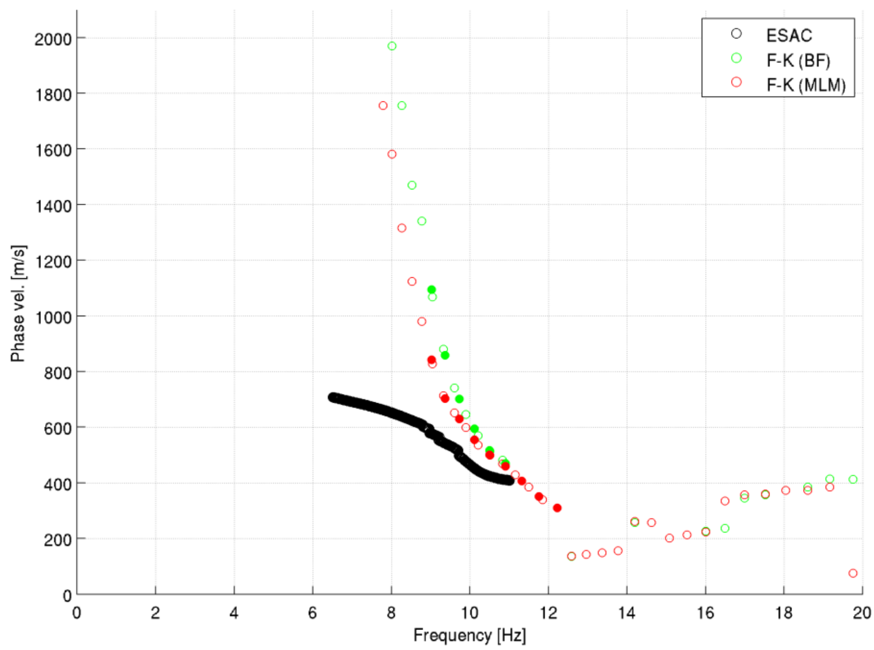

Figure 16: Comparison of experimental phase velocity estimated by the ESAC and the F-K (for both Beam Forming and Maximum-Likelihood Method) methods; filled circles represent values potentially used for inversions.

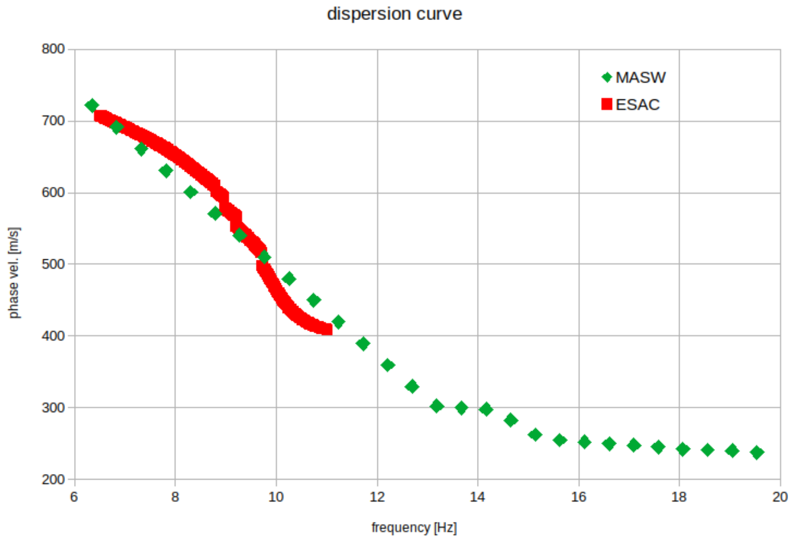

Figure 17: Comparison of experimental phase velocity estimated by the ESAC method and the MASW survey.

B2. SEISMIC VELOCITY MODEL

The non-linear inversions are performed using the software *joinv6* (Parolai *et al.*, 2005; Giustiniani *et al.*, 2020), which adopt a genetic algorithm (Yamanaka and Ishida, 1996). The forward modelling of Rayleigh wave phase velocities and HVSR curves is performed under the assumption of a vertically heterogeneous 1D Earth model using the modified Thomson-Haskell method proposed by Wang (1999) and following the suggestions of Arai and Tokimatsu (2004) and Tokimatsu *et al.* (1992). The modelling is not restricted to the fundamental mode, preserving the possibility that higher modes participate in simulating the observed dispersion and HVSR curves.

The experimental dispersion curve used as input for inversions is the one estimated from the ESAC analysis in the frequency interval 6.5-11 *Hz*, plus that obtained from the MASW survey in the frequency interval 11-20 *Hz*. The experimental HVSR is used between about 3 and 10 *Hz*. In the left panel of Figure 18 tested models are shown in different colors according to their cost value: the more reliable model (minimum cost) is in white, the models lying inside the 10% range of the minimum cost are in black and the other tested models are shown in grey. In the right-central and right-bottom panels of Figure 18, the agreement between experimental and theoretical (grey and open circles, respectively) Rayleigh-wave dispersion curves and HVSR are shown. The agreement is good and, considering the wavelengths related to the dispersion curve frequency range, the V_S profile between about 5-50 *m* is very well constrained. Table 5 reports the minimum-cost shear-wave velocity model.

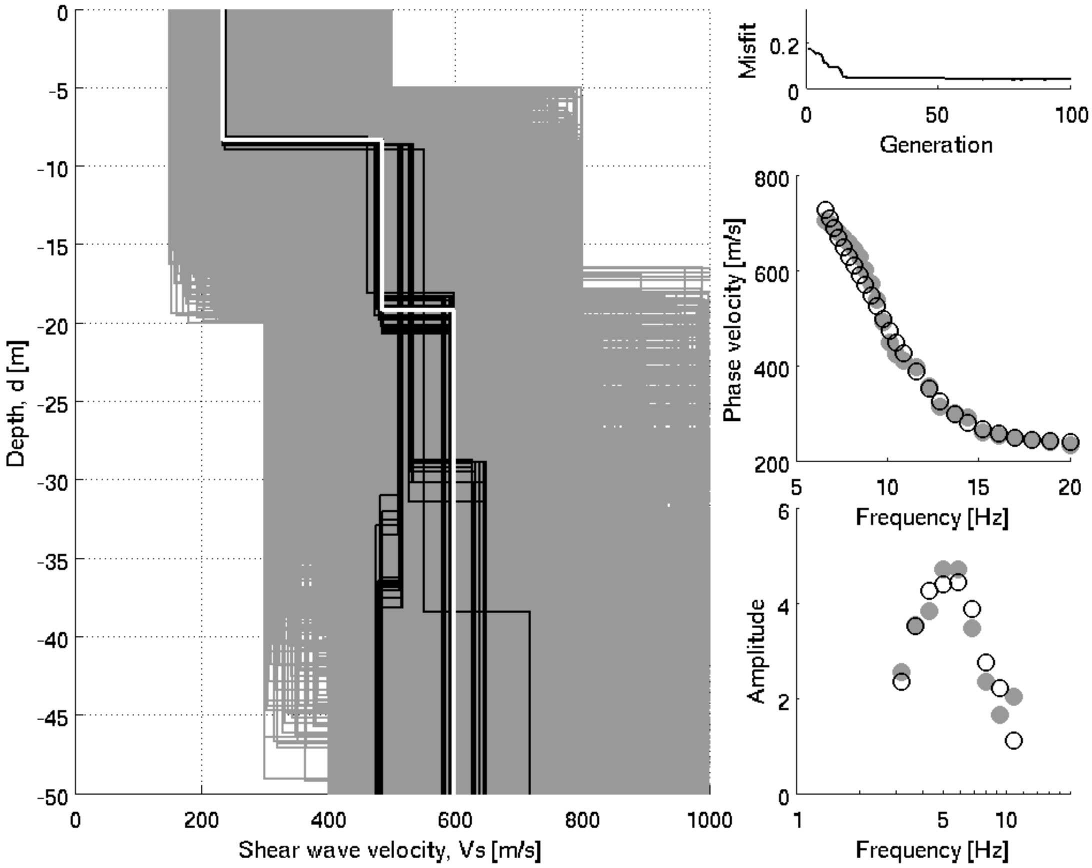

Figure 18: Shear-wave velocity models modeled during the inversion procedure (left panel): tested models (grey lines), the minimum cost model (white line) and models lying inside the minimum cost + 10% range (black lines); the generation values versus misfit (right-upper panel); the fitting of experimental data (grey circles) and empirical values relative to the minimum cost model (white circles) relevant to the dispersion curve (right-central panel) and to HVSR (right-bottom panel).

Table 5: Best-fit shear-wave velocity model

From [*m*]	To [*m*]	Thickness [*m*]	V_S [*m/s*]
0	8.3	8.3	234
8.3	19	10.7	484
19	-	-	598

B3. CONCLUSIONS

As evinced from results of geophysical investigations carried out by INGV Working Group, we can attribute to the shallower layer (represented by the Villa Verucchio Subsynthem) a V_S value of 234 *m/s*, and to the Dovadola Member V_S values from 484 to 598 *m/s*, compatible with EC8 class assigned at the site according to geological evidences.

According to the current Italian seismic code (NTC18), if the bedrock (V_S > 800 *m/s*) is more than 30 *m* in depth, the equivalent velocity ($V_{S,eq}$) is equal to the $V_{S,30}$. From Figure 18, the velocity of 800 *m/s* is reached for an unknown depth, well below the depth of 30 *m*.

Therefore, in this case, both $V_{S,eq}$ and $V_{S,30}$ are equal to 395 *m/s*. Of consequence, IT.BRH site is classified in the soil category B, for both the NTC18 and EC8 seismic codes (Table 6).

Table 6: $V_{S,eq}$, $V_{S,30}$ and soil classes

$V_{S,eq}$ = $V_{S,30}$ [*m/s*]	Soil class (NTC18)	Soil class (EC8)
395	B	B

ACKNOWLEDGEMENTS

Authors wish to thank Stefano Parolai, Paolo Bernardi and Ilaria Dreossi (Istituto Nazionale di Oceanografia e di Geofisica Sperimentale – OGS), for providing us the software "joinv6", which has been adopted as inversion procedure to estimate the shear-wave velocity model, and for the precious guide in its usage.

REFERENCES

Aki K. (1957). “Space and time spectra of stationary stochastic waves, with special reference to microtremors”, Bulletin of the Earthquake Research Institute, 35, pp. 415–456.

Amanti M., Battaglini L., Campo V., Cipolloni C., Congi M. P., Conte G., Delogu D., Ventura R., Zonetti C. (2008). “The Lithological map of Italy at 1:100.000 scale: An example of re-use of an existing paper geological map”, 33rd International Geological Conference, IEI02310L – 6-14th August, Oslo (Norway).

APAT – Geological Survey of Italy – Geological Map of Italy 1:50.000 (CARG Project) – https://www.isprambiente.gov.it/Media/carg/239_FAENZA/Foglio.html.

Arai H. and Tokimatsu K. (2004). “S-wave velocity profiling by inversion of microtremor H/V spectrum”, Bulletin of the Seismological Society of America, 94, pp. 53–63.

Capon J. (1969). “High-resolution frequency-wavenumber spectrum analysis”, Proceedings of the IEEE, 57, pp. 1408–1418.

Comune di Brisighella (2019). Microzonazione Sismica del Comune di Brisighella (Livello 3) – Relazione illustrativa.

EC8: European Committee for Standardization (2004). Eurocode 8: design of structures for earthquake resistance. P1: General rules, seismic actions and rules for buildings. Draft 6, Doc CEN/TC250/SC8/N335.

Foti S., Parolai S., Albarello D., *et al.* (2009). Deliverable 6: Application of surface wave methods for seismic site characterization. DPC-INGV S4 Project 2007-2009 (http://esse4.mi.ingv.it) – last accessed in June 2021 at http://esse4.mi.ingv.it/files/images/stories/deliverable_d6.pdf.

Foti S., Parolai S., Albarello D., *et al.* (2010). Deliverable 7: Application of surface wave methods for seismic site characterization of ITACA stations. DPC-INGV S4 Project 2007-2009 (http://esse4.mi.ingv.it) – last accessed in June 2021 at http://esse4.mi.ingv.it/files/images/stories/deliverable_d7.pdf.

Foti S., Hollender F., Garofalo F., *et al.* (2017). "Guidelines for the good practice of surface wave analysis: a product of the InterPACIFIC project", Bull Earthquake Eng, 16, pp. 2367-2420.

Giustiniani M., Tinivella U., Parolai S., Donda F., Brancolini G., Volpi V. (2020). "Integrated Geophysical Analyses of Shallow-Water Seismic Imaging With Scholte Wave Inversion: The Northern Adriatic Sea Case Study", Frontiers in Earth Science, vol. 8, p. 532, https://www.frontiersin.org/article/10.3389/feart.2020.587898 doi:10.3389/feart.2020.587898.

Lacoss R.T., Kelly E.J. and Toksöz M.N. (1969). "Estimation of seismic noise structure using arrays", Geophysics, 34, pp. 21–38.

Lugli S., Manzi V., Roveri M. (2015). "Geologia dei Gessi di Brisighella e Rontana", I Gessi di Brisighella e Rontana, Memorie dell'Istituto Italiano di Speleologia, s. II, 28, pp. 17-26.

Montanari D., Del Ventisette C., Bonini M., Sani F. (2007). "Passive-roof thrusting in the Messinian Vena del Gesso Basin (Northern Apennines, Italy): constraints from field data and analogue models", Geological Journal, 42, pp. 455-476.

NTC 2018: Ministero delle Infrastrutture e dei Trasporti (2018). Aggiornamento delle Norme Tecniche per le Costruzioni. Part 3.2.2: Categorie di sottosuolo e condizioni topografiche, Gazzetta Ufficiale n. 42 del 20 febbraio 2018 (in Italian).

Ohori M., Nobata A. and Wakamatsu K. (2002). "A comparison of ESAC and FK methods of estimating phase velocity using arbitrarily shaped microtremor analysis", Bulletin of the Seismological Society of America, 92, pp. 2323–2332.

Okada H. (2003). The Microtremor Survey Method. SEG

Parolai S., Picozzi M., Richwalski S.M. and Milkereit C. (2005). "Joint inversion of phase velocity dispersion and H/V ratio curves from seismic noise recordings using a genetic algorithm, considering higher modes", Geophysical Research Letters, 32, L01303. doi:10.1029/2004GL021115.

Parolai S., Richwalski S.M., Milkereit C. and Fäh D. (2006). "S-wave velocity profile for earthquake engineering purposes for the Cologne area (Germany)", Bulletin of the Earthquake Research Institute, 4, pp. 65–94. doi:10.1007/s10518-005-5758-2.

PCM-DPC (1972). Italian Strong Motion Network. Presidency of Council of Ministers (PCM) - Civil Protection Department (DPC). https://doi.org/10.7914/SN/IT.

Regione Emilia Romagna – Geoportale - https://geoportale.regione.emilia-romagna.it/it.

Roveri M., Manzi V., Ricci Lucchi F., Rogledi S. (2003). "Sedimentary and tectonic evolution of the Vena del Gesso basin (Northern Apennines, Italy): Implications for the onset of the Messinian salinity crisis", Geological Society of America Bulletin, v. 115, no. 4, pp. 387-405.

Simoni A., Elmi C., Picotti V. (2003). "Late Quaternary uplift and valley evolution in the Northern Apennines: Lamone catchment", Quaternary International 101-102, pp. 253-267.

Technical Commission SM, 2015 – Microzonazione sismica. Standard di rappresentazione e archiviazione informatica, Versione 4.0b (Commissione tecnica inter-istituzionale per la MS nominata con DPCM 21 aprile 2011).

Tokimatsu K., Tamura S. and Kojima H. (1992). "Effects of multiple modes on Rayleigh wave dispersion characteristics", Journal of Geotechnical Engineering, 118, pp. 1529–1543.

Wang R. (1999). "A simple orthonormalization method for stable and efficient computation of Green's functions", Bulletin of the Seismological Society of America, 89, pp. 733–741.

Yamanaka H. and Ishida H. (1996). "Application of generic algorithms to an inversion of surface-wave dispersion data", Bulletin of the Seismological Society of America, 86, pp. 436–444.

Disclaimer and limits of use of information

This study has benefited from funding provided by the Italian Presidenza del Consiglio dei Ministri – Dipartimento della Protezione Civile (DPC). This paper does not necessarily represent DPC official opinion and policies.

Esclusione di responsabilità e limiti di uso delle informazioni

Lo studio presentato ha beneficiato del contributo finanziario della Presidenza del Consiglio dei Ministri – Dipartimento della Protezione Civile; la presente pubblicazione, tuttavia, non riflette necessariamente la posizione e le politiche ufficiali del Dipartimento.

[1]This document is level 3 as defined in the "Principi della politica dei dati dell'INGV (D.P. n. 200 del 26.04.2016)"